PHYSICAL REVIEW A **88**, 053614 (2013)

Effects of interaction on thermodynamics of a repulsive Bose-Einstein condensate

Satadal Bhattacharyya,[1] Tapan Kumar Das,[2,*] and Barnali Chakrabarti[3]
[1]*Department of Physics, Scottish Church College, 1 and 3 Urquhart Square, Kolkata 700006, India*
[2]*Department of Physics, University of Calcutta, 92 A. P. C. Road, Kolkata 700009, India*
[3]*Department of Physics, Kalyani University, Kalyani, Nadia, West Bengal 741235, India*
(Received 29 July 2013; published 13 November 2013)

We report the effects of interaction on thermodynamic properties of a repulsive Bose-Einstein condensate confined in a harmonic trap by using the correlated potential harmonics expansion method. This many-body technique permits the use of a realistic interactomic interaction, which gives rise to the effective long-range interaction of the condensate in terms of the s-wave scattering length. We have computed temperature (T) dependence of the chemical potential, specific heat, condensate fraction, entropy, pressure, and the average energy per particle of a system containing a large number (A) of ^{87}Rb atoms in the Joint Institute for Laboratory Astrophysics (JILA) trap. The repulsion among the interacting bosons results in a small but measurable drop of condensate fraction and critical temperature (T_c), compared to those of a noninteracting condensate. These are in agreement with the experiment. Although all thermodynamic quantities have a strong dependence on A and to a smaller extent on the interatomic interaction, our numerical calculation appears to show that a thermodynamic quantity per particle follows a universal behavior as a function of T/T_c. This shows the importance of T_c for all thermodynamic properties of the condensate. As expected, for $T > T_c$, these properties follow those of a trapped noncondensed Bose gas.

DOI: 10.1103/PhysRevA.88.053614 PACS number(s): 03.75.Hh, 31.15.xj, 03.65.Ge, 03.75.Nt

I. INTRODUCTION

Since the achievement of the Bose-Einstein condensation (BEC) in dilute vapors of alkali-metal atoms, there has been a flurry of activities on BEC, both experimental [1–4] as well as theoretical [5–8], highlighting the importance of studying various properties [5–10] of interacting bosons confined in an external potential trap. However, most of these works have been focused on the static and zero-temperature aspects of the condensates. Much less attention has been paid to the theoretical study of different thermodynamic properties because such studies require a large number of energy levels of the condensate, involving extremely computer-intensive calculations. This is true even for the mean-field Gross-Pitaevskii (GP) equation. For an essentially exact many-body technique like the diffusion Monte Carlo (DMC) method [11], such calculations are much heavier. On the other hand, analytical expressions can be obtained for noninteracting bosons, assuming the number (A) of trapped bosons to be very large [5,6]. Effects of finite size (finite A) were estimated to be small for $A > 10^4$ noninteracting bosons [5]. But the effect of atom-atom interactions is quite important even in a typical *dilute* condensate, for which $n|a_s|^3 \ll 1$, where n is the number density and a_s is the s-wave scattering length. The parameter expressing the importance of interaction energy compared to the kinetic energy is $A|a_s|/a_{ho}$ [5], with a_{ho} being the harmonic oscillator length. Thus for the original JILA experiment [2] with $A = 40\,000$ and $a_s/a_{ho} = 0.004\,33$, the effect of interactions is quite significant, even though the condensate is very dilute. Moreover, the strong central peak has a higher density than the outer regions. Hence, smaller average pair separation for condensed particles enhances the effect of atom-atom interaction for $T < T_c$. On the other hand, for $T > T_c$, average interatomic separation is much larger than the range of two-body interaction and the effect of interaction on the noncondensed Bose gas is negligible. Moreover, the finite-size effect may be pushed up to larger A in the presence of interaction, since the net interaction increases as the number of pairs. It is already known that interatomic interaction produces an appreciable effect on the energy, density profile, and some other static properties of even a dilute condensate [5,12]. Thus one may expect *a priori* an appreciable effect of interatomic interaction on the thermodynamics of a condensate.

In this communication, we focus our attention on the less explored domain of BEC thermodynamics, with particular emphasis on the effect of interatomic interactions through a many-body treatment. For this purpose, we use the correlated potential harmonics expansion (CPHE) technique [12,13]. The CPHE method is an approximate but *ab initio* many-body theory, particularly suited to dilute BEC, where correlations higher than two-body ones can be safely disregarded [13]. Due to freezing of irrelevant degrees of freedom, the computational technique is quite manageable, even for large A (for details, see the next section). This method has been established over the past few years as a simple but powerful technique to study dilute BEC. It has been used successfully to study different aspects of BEC, *viz*., its ground-state properties and low-lying collective excitations at $T = 0$. An advantage of the CPHE method is that it produces an effective potential in the hyper-radial space, in which the condensate executes collective motions as a single quantum entity. Thus, calculating the excited states of the system is relatively simple. Recently the CPHE method has also been used to calculate the heat capacity of an attractive condensate [14] containing a fixed number of ^{7}Li atoms. For an attractive interaction the number of atoms is limited by an upper bound, *viz.*, the critical number, beyond which the condensate collapses. On the other hand, the number of atoms in a repulsive condensate can be quite large. Due to numerical limitations, the original CPHE method was computationally possible for A up to $\sim$15 000. Although the upper limit of A has been pushed up using a mathematical

---

[*] Corresponding author: kumartd@rediffmail.com

limiting relation for static properties [15], in this work, we restrict ourselves to $5\,000 \leqslant A \leqslant 15\,000$ trapped ^{87}Rb atoms to study the temperature dependence of several thermodynamic observables of the repulsive condensate. The number is comparable with the JILA experiment [2], but small enough so that the finite-size effect may show up. We find that the general pattern of the experimental results is fairly well reproduced in our calculation. Comparing with earlier estimates obtained from approximate solutions of the GP equation [5] and also with path integral Monte Carlo calculations [16], we find that our results are in the same range, but closer to experimental ones, for T not too close to T_c. These show that the effect of interactions on thermodynamics of the repulsive JILA condensate is non-negligible but relatively weak. This can be understood as follows. For $T < T_c$, only a few particles are in states other than the ground state. The occupation of such states is given by the Bose distribution, depending on the difference of energy of the levels and the chemical potential $\mu(T)$. The latter is slightly smaller than the ground-state energy. It was found earlier that energies of the ground and excited states depend strongly on interaction [12], while excitation energies depend weakly on interaction for repulsive condensates [17]. This will affect $\mu(T)$, as also energies of all the levels strongly but their difference weakly. Since only a microscopic fraction of the particles occupy the excited states, total energy of the system at T *not too close to* T_c does not depend too strongly on the interatomic interaction. Thus the thermodynamic parameters (except the energy per particle) are less strongly dependent on the atom-atom interaction than the energies of the ground and excited states.

We also observe that although the critical temperature (T_c) and all the thermodynamic parameters of the system depend on the number of trapped bosons and to a smaller extent on the interatomic interaction, a thermodynamic quantity *per particle* in a dimensionless form appears to be a universal function of T/T_c only (the only exception being the energy per particle of the *noninteracting* condensate, which is appreciably lower than that of the interacting condensate, as it follows from the foregoing discussion). Thus by knowing T_c for a particular configuration of the condensate and a knowledge of the universal function for a particular thermodynamic parameter, one can get that thermodynamic quantity per particle as a function of temperature T. Such information is quite useful because a direct experimental measurement is usually very difficult. This observed characteristic for the finite interacting systems corresponds to the scaling behavior reported earlier [5,18].

The plan of the paper is as follows. In Sec. II A the potential harmonics expansion method is briefly outlined for convenience in reading and definition of symbols used. In Sec. II B the numerical scheme for calculation of thermodynamic properties of ^{87}Rb condensate is presented. The results and discussion are presented in Sec. III and finally in Sec. IV we present our concluding remarks after a brief summary.

II. FORMALISM

A. Correlated potential harmonics expansion (CPHE) technique

In this subsection, we briefly discuss the correlated potential harmonics expansion (CPHE) method adopted for the approximate solution of the many-body Schrödinger equation for the dilute Bose condensates. Since this technique is already well established and documented, we only present a brief outline in the following. Interested readers can find the details in Refs. [12,13,19].

The relative motion of a system of A identical bosons of mass m confined by an external trap V_{trap} is given by

$$\left[-\frac{\hbar^2}{m}\sum_{i=1}^{N}\nabla^2_{\vec{\zeta}_i} + V_{\text{trap}}(\vec{\zeta}_1,\ldots,\vec{\zeta}_N) + V(\vec{\zeta}_1,\ldots,\vec{\zeta}_N) - E_R\right] \times \psi(\vec{\zeta}_1,\ldots,\vec{\zeta}_N) = 0, \tag{1}$$

where $\{\zeta_1,\ldots,\zeta_N\}$ is a set of $N = A-1$ Jacobi vectors [20] and E_R is the energy of relative motion. The hyperspherical variables consist of a hyperradius

$$r = \left[\sum_{i=1}^{N}\zeta_i^2\right]^{\frac{1}{2}}, \tag{2}$$

and $(3N-1)$ hyperangles constituted by the polar angles of N Jacobi vectors and $N-1$ angles defining the relative lengths of these Jacobi vectors [20]. The hyperspherical harmonics expansion method (HHEM) consists of expanding ψ, in the complete set of hyperspherical harmonics (HH), which are the eigenfunctions of the N-dimensional hyperangular momentum operator. Substitution of this expansion in Eq. (1) and projection on a particular HH give rise to a set of coupled differential equations (CDE). This straightforward procedure becomes difficult as A increases beyond 3, due to the very rapid increase in the degeneracy of HH basis [20]. Note that this basis incorporates all many-body correlations.

However, for a dilute BEC a great simplification is possible. The bosons in the condensate have extremely low energies ($\sim 10^{-13}$ eV), so that the two-body scattering is described completely by the s-wave scattering length (a_s), and $|a_s|$ becomes the range of the effective interaction. This *effective interaction for the BEC* can be attractive or repulsive, according to whether a_s is negative or positive, although the *actual interatomic interaction* has an attractive tail $-C_6/r_{ij}^6$ of the van der Waals potential (r_{ij} being the separation of the (ij) pair) [6], with a range $\sim$10 Bohr. The average pair separation in a dilute BEC is much larger than $|a_s|$, and the pair feels the effective potential. However, if r_{ij} were small compared to $|a_s|$, the interacting pair would feel the strong van der Waals attraction (even in a repulsive condensate) and could form a bound state. Now a binary molecule formation is possible only through three-body collisions, so that the third particle flies away with the released binding energy. In order to eliminate depletion of the BEC through molecule formation, the density of a laboratory BEC is designed to be so low that the average pair separation is much larger than $|a_s|$, i.e., $n|a_s|^3 \ll 1$ is satisfied, where n is the number density [5]. Now, $n \sim A/a_{ho}^3$, where $a_{ho} = \sqrt{\hbar/(m\omega)}$ is the oscillator length of the trap of frequency $\nu = \omega/2\pi$. Hence this condition is $A|\frac{a_s}{a_{ho}}|^3 \ll 1$. For the ^{87}Rb condensate $a_s = 100$ Bohr and for the JILA trap, $\frac{a_s}{a_{ho}} = 0.004\,33$. For $A \leqslant 15\,000$, this condition is well satisfied.

Because of the extreme diluteness of the condensate and the lack of three-body collisions, only two-body correlations in ψ are relevant and the latter can be decomposed in Faddeev components ψ_{ij} for the (ij)-interacting pair, which becomes a function of the pair separation $\vec{r}_{ij}$ and r only [21]

$$\psi = \sum_{i,j>i}^{A} \psi_{ij}(\vec{r}_{ij},r). \tag{3}$$

Clearly then $\psi_{ij}(\vec{r}_{ij},r)$ can be expanded in a subset of HH, called the potential harmonics (PH) subset. This subset is sufficient for the expansion of the interaction potential $V(\vec{r}_{ij})$ as a function in the hyperangular space. A simple analytic expression for the potential harmonic $\mathcal{P}^{lm}_{2K+l}(\Omega^{ij}_{N})$ is possible [21]. Here, l and m are the orbital angular momentum of the system and its projection and K is the $3N$-dimensional grand orbital quantum number. Expansion of the Faddeev component in the PH basis is given as

$$\psi_{ij}(\vec{r}_{ij},r) = r^{-\frac{(3N-1)}{2}} \sum_{K} \mathcal{P}^{lm}_{2K+l}\big(\Omega^{(ij)}_{N}\big) u^{l}_{K}(r)\eta(r_{ij}). \tag{4}$$

An additional short-range correlation function $\eta(r_{ij})$ is included to improve the convergence of the basis [12]. It is chosen to be the zero-energy solution of the two-body Schrödinger equation

$$-\frac{\hbar^2}{m}\frac{1}{r_{ij}^2}\frac{d}{dr_{ij}}\left(r_{ij}^2\frac{d\eta(r_{ij})}{dr_{ij}}\right) + V(r_{ij})\eta(r_{ij}) = 0, \tag{5}$$

which has the same short-range behavior as $\psi_{ij}(\vec{r}_{ij},r)$. The asymptotic form of $\eta(r_{ij})$ is given in terms of a_s as $C(1-\frac{a_s}{r_{ij}})$ [6]. The short-separation behavior of $V(r_{ij})$ (such as the hard core radius of the van der Waals potential) can be adjusted to correspond to the experimental a_s value. Substitution of the expansion, Eq. (4), in the Faddeev equation and projection on the PH for the (ij)-partition give [12]

$$\begin{aligned}\bigg\{&-\frac{\hbar^2}{m}\frac{d^2}{dr^2} + \frac{\hbar^2}{mr^2}[\mathcal{L}(\mathcal{L}+1) + 4K(K+\alpha+\beta+1)] \\ &+ V_{\text{trap}}(r) - E_R\bigg\} U_{Kl}(r) + \sum_{K'} f_{Kl}V_{KK'}(r)f_{K'l}U_{K'l}(r) = 0,\end{aligned} \tag{6}$$

where $U_{Kl}(r) = f_{Kl}u^{l}_{K}(r), \mathcal{L} = l + \frac{3A-6}{2}, \alpha = \frac{3A-8}{2}, \beta = l + \frac{1}{2}$, with l being the orbital angular momentum of the system contributed by the interacting pair. The constant f^2_{Kl} is the overlap of the PH for interacting partition with the sum of the full set of PH for all partitions. An expression in a closed form can be found in Ref. [21]. The resulting potential matrix element $V_{KK'}(r)$ is [12]

$$\begin{aligned}V_{KK'}(r) = \big(h^{\alpha\beta}_{K}h^{\alpha\beta}_{K'}\big)^{-\frac{1}{2}} \int_{-1}^{+1} \bigg[P^{\alpha\beta}_{K}(z)V\left(r\sqrt{\frac{1+z}{2}}\right) \\ \times P^{\alpha\beta}_{K'}(z)\eta\left(r\sqrt{\frac{1+z}{2}}\right)W_l(z)\bigg]\,dz,\end{aligned} \tag{7}$$

where $h^{\alpha\beta}_{K}$ and $W_l(z)$ are respectively the norm and weight function of the Jacobi polynomial $P^{\alpha\beta}_{K}(z)$ [22]. Inclusion of the short-range correlation function, $\eta(r_{ij})$, makes the PH basis nonorthogonal. Standard procedure for handling nonorthogonal basis can be followed. However, dependence of the overlap $\langle\mathcal{P}^{lm}_{2K+l}(\Omega^{(ij)}_{N})|\mathcal{P}^{lm}_{2K'+l}(\Omega^{(kl)}_{N})\eta(r_{kl})\rangle$ on the hyper-radius r makes this very involved. On the other hand, actual numerical calculation shows that this overlap matrix is nearly a constant times the unit matrix, except for a very narrow interval of small r values. Disregarding its derivatives, we approximately get Eq. (6), with effective potential matrix element given by Eq. (7) [23]. One notices that the effective two-body interaction becomes $V(r_{ij})\eta(r_{ij})$. One can understand this physically as follows. Since the interacting atoms in the BEC have very low energy, a pair of them do not come close enough to "see" the *actual* interatomic interaction (note that $\eta(r_{ij})$ is vanishingly small for small values of r_{ij} [19]). Thus the *effective interaction seen by the pair* is governed by a_s through $\eta(r_{ij})$.

This procedure reduces algebraic and numerical complexities drastically, since the number of active degrees of freedom reduces to only *four* for a particular (ij)-partition, with the remaining unimportant ones being "frozen". This permits us to solve the system up to $A = 15\,000$. For larger A, the quantity α becomes too large to be handled by the computer, especially for the weight function $W_l(z)$ of the Jacobi polynomial [12]. The CPHE technique has been successfully applied to study $T=0$ properties of both repulsive and attractive condensates [12,13,24].

To solve Eq. (6) we adopt the hyperspherical adiabatic approximation (HAA) [25], instead of a numerical algorithm for solving CDE, for simplicity as well as for a better physical insight, as discussed below. In HAA, the hyperradial motion is adiabatically separated from the hyperangular motion, assuming the former is much slower than the latter. This assumption is justified, since the hyper-radial motion corresponds to the breathing mode. It has been tested to be accurate to better than 1% for both nuclear and atomic systems [26]. The hyperangular motion is solved by diagonalizing the potential matrix, together with the hypercentrifugal repulsion for a fixed value of r. The lowest eigenvalue, called the lowest eigenpotential $\omega_0(r)$, is used in the adiabatically separated uncoupled hyper-radial differential equation

$$\left[-\frac{\hbar^2}{m}\frac{d^2}{dr^2} + \omega_0(r) - E_R\right]\zeta_0(r) = 0 \tag{8}$$

to obtain E_R and the hyperadial wave function $\zeta_0(r)$ in the extreme adiabatic approximation (EAA) [25]. Besides simplifying calculations, the HAA provides a physical insight in terms of an effective potential, $\omega_0(r)$, for the hyper-radial motion, while the structure of the condensate is obtained in terms of $\zeta_0(r)$. We solve Eq. (8) by the Runga-Kutta method, subject to appropriate boundary conditions to get E_R and $\zeta_0(r)$. The center-of-mass energy is added to each energy eigenvalue to obtain the energy levels E_{nl}. To avoid the serious numerical difficulty in evaluating $W_l(z)$ for $l>0$, we take the potential matrix element (which does not change much with l) for $l=0$ and add the hypercentrifugal repulsion (HCR) term corresponding to the chosen value of l. For calculation of E_{nl}, contribution of HCR is important only near the minimum of the well in $\omega_0(r)$. The contribution of ordinary centrifugal repulsion (due to l) is bundled together with the "hypercentrifugal part" due to hyper angular momentum, in Eq. (6). In a noninteracting condensate, the minimum of $\omega_0(r)$ occurs at $r_{\text{min}} \simeq \sqrt{3A}$, and the effect of ordinary centrifugal repulsion is correctly taken. But in a repulsive condensate, the minimum of

$\omega_0(r)$ occurs at a value of $r_{\min} \gg \sqrt{3A}$ for large A, since $r_{\min}$ increases due to $A(A-1)/2$ pairwise repulsions. Since the contributions of both ordinary and hypercentrifugal repulsions decrease as r^{-2} in Eq. (6), the effective contribution due to ordinary centrifugal repulsion becomes quite small for large A. Hence E_{nl} for $l > 0$ becomes appreciably lower than what it should have been. We have corrected for this empirically by taking the contribution of the ordinary centrifugal repulsion corresponding to the appropriate r values. Note that energies of $l = 0$ states (E_{n0}) are not affected.

For the interatomic potential, we choose the commonly used realistic van der Waals (vdW) potential, whose short-range repulsion is modeled by a hard core of radius r_c [6]

$$\begin{aligned} V(r_{ij}) &= \infty \qquad \text{for } r < r_c \\ &= -\frac{C_6}{{r_{ij}}^6} \qquad \text{for } r_{ij} \geqslant r_c, \end{aligned} \tag{9}$$

which has the well-known r_{ij}^{-6} attractive tail. The value of C_6 is known for a particular type of atoms and r_c is adjusted to reproduce experimental a_s in the asymptotic form of $\eta(r_{ij})$ [6]. This ensures that the correct effective two-body interaction, expressed in terms of a_s, has been taken.

B. Calculation of thermodynamic quantities

The number of bosons in the energy level E_{nl} at a temperature $T > 0$ is given by the Bose distribution function

$$f(E_{\mathrm{nl}}) = \frac{1}{e^{\beta(E_{\mathrm{nl}}-\mu)} - 1}, \tag{10}$$

where $\beta = 1/k_BT$ and μ is the chemical potential, obtained from

$$A = \sum_{n=0}^{\infty}\sum_{l=0}^{\infty}(2l+1)f(E_{\mathrm{nl}}). \tag{11}$$

Clearly μ is a function of T. At $T = 0$, μ is equal to the ground-state energy and all the bosons occupy this level. The total energy of the condensate at a temperature T is

$$E(A,T) = \sum_{n=0}^{\infty}\sum_{l=0}^{\infty}(2l+1)f(E_{\mathrm{nl}})E_{\mathrm{nl}}. \tag{12}$$

The specific heat of the condensate for a fixed particle number is

$$C_A(T) = \left.\frac{\partial E(A,T)}{\partial T}\right|_A, \tag{13}$$

which can be calculated using Eqs. (10), (12), and (13) [14]. In the usual textbook treatment in the thermodynamic limit [27], μ is taken to remain equal to the ground-state energy for $T \leqslant T_c^0$, where T_c^0 is the critical temperature in the thermodynamic limit. Bose condensation takes place at $T < T_c^0$. In this treatment, the sums in Eqs. (11) and (12) are replaced in the semiclassical approximation by integrals over energy, assuming a continuous energy spectrum and a closed expression for T_c^0 can be given. But for finite A in the harmonic trap, assumption of a continuous energy spectrum is not valid. Exact numerical evaluation of the sum shows that μ depends on T for all T: It decreases *very slowly* from its value E_{00} at $T = 0$, for T less than a particular value T_c, and then it decreases *rapidly* for $T > T_c$. In this case, the critical temperature is not well defined and no analytic expression is possible for T_c. Instead, one notices that $C_A(T)$ increases to a maximum at $T = T_c$ and then falls to its asymptotic value of $3k_BA$ for large T [28]. We follow the definition of *transition temperature* T_c [28] to be the temperature at which $C_A(T)$ is a maximum

$$\left.\frac{\partial C_A(T)}{\partial T}\right|_{T_c} = 0. \tag{14}$$

It is seen that as $A \to \infty$, T_c approaches T_c^0, for noninteracting bosons [28]. In our numerical procedure, we calculate a large number of energy levels E_{nl}, with n and l running typically from 0 to 300 and 0 to 200 respectively. Using these values and a chosen upper energy limit E^u, all energy levels $E_{\mathrm{nl}} < E^u$ are included in Eq. (11) to solve for μ. We next increase E^u and repeat the process, until μ converges for a particular temperature. This value of μ and E^u are used for calculation of $C_A(T)$, condensate fraction (defined as the number of atoms in the ground state divided by A), and other thermodynamic quantities.

The entropy of the system is calculated using the standard relation for bosons [6]

$$S = k_B\sum_{\mathrm{nl}}\{[1+f(E_{\mathrm{nl}})]\ln[1+f(E_{\mathrm{nl}})] - f(E_{\mathrm{nl}})\ln f(E_{\mathrm{nl}})\}. \tag{15}$$

Finally, the pressure is calculated (in terms of the dimensionless quantity $\frac{PV}{k_BT}$, V being the volume of the condensate) using the relation of grand partition function

$$\frac{PV}{k_BT} = -\sum_{\mathrm{nl}}\ln(1 - \mathrm{e}^{-\beta(E_{\mathrm{nl}}-\mu)}). \tag{16}$$

III. RESULTS AND DISCUSSION

We perform the calculations for chosen values of A in a condensate of ^{87}Rb atoms having s-wave scattering length $a_s = 0.004\,33\ a_{\mathrm{ho}}$, corresponding to the original JILA experiment [2], and assume a spherically symmetric harmonic trap of frequency of $\omega = 2\pi \times 77.78$ Hz. In order to compare with the noninteracting case for a finite value of A, we use the procedure and relations of Sec. II B with the noninteracting energy values $E_{\mathrm{nl}} = 2n + l$.

In Fig. 1, we plot μ/μ_0 calculated by the CPHE method as a function of T (in nK) for $A = 5\,000, 10\,000$, and $15\,000$ (continuous red [gray] curves labeled by 2,4, and 6 respectively), where μ and μ_0 are the chemical potentials at temperatures T and 0 respectively. For comparison we also plot the noninteracting results for the same values of A (dotted blue [gray] curves, labeled by 1,3, and 5 respectively). It is seen that both the interacting and noninteracting bosons have the same general features. Below a certain transition temperature T_c (calculated later in the text), μ/μ_0 decreases very slowly for both interacting and noninteracting bosons, remaining almost constant. This is close to the prediction of the textbook treatment in the thermodynamic limit ($A \to \infty$). Beyond T_c, μ/μ_0 decreases rapidly. One can also see from Fig. 1 that the fall in μ/μ_0 is rapid for smaller A and gradually becomes slower for larger A. However, μ decreases more rapidly with T for larger A, since μ_0 (which is equal to the ground-state

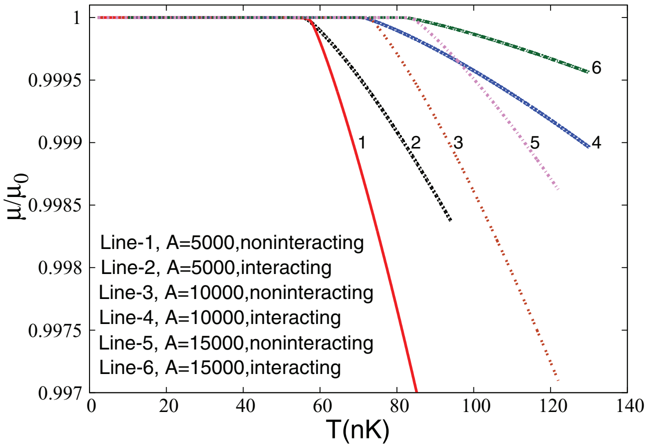

FIG. 1. (Color online) Plot of calculated μ/μ_0 against T in nK for A bosons in the harmonic trap by the CPHE method. Curves labeled by 2, 4, and 6 are for $A = 5\,000, 10\,000$, and $15\,000$ interacting bosons respectively. μ/μ_0 for noninteracting bosons are also plotted for comparison for the same values of A as curves labeled by 1, 3, and 5 for $A = 5\,000, 10\,000$, and $15\,000$ respectively.

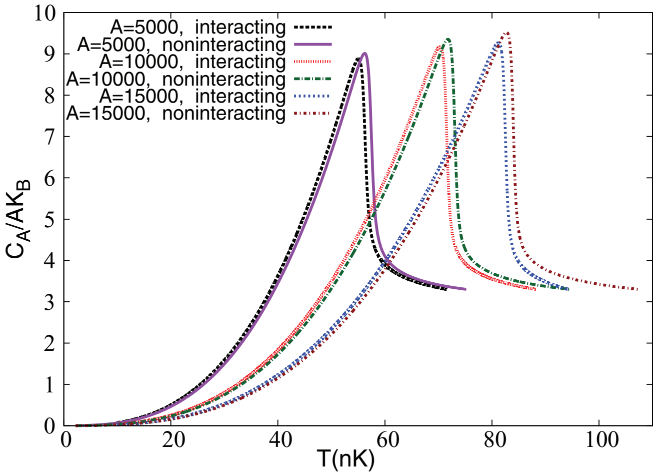

FIG. 2. (Color online) Plot of $C_A(T)/Ak_B$ against T in nK for indicated number of bosons in the harmonic trap. Results for noninteracting bosons are also included. The left, middle, and right pairs of closely spaced curves correspond to $A = 5\,000$, $10\,000$, and $15\,000$ respectively. For each closely spaced pair, the left curve is for interacting bosons, while the right one is for noninteracting bosons. It is seen that the repulsive interaction lowers T_c and the effect increases with A. Also the fall in C_A/Ak_B for $T > T_c$ becomes sharper with increase in A.

energy) increases rapidly with A. The fact that for $T < T_c$, the chemical potential is almost equal to μ_0 indicates that below T_c, a macroscopic fraction of the particles reside in the ground state. We find that μ/μ_0, for both interacting and noninteracting condensate, depend strongly on A for $T > T_c$. In this temperature range, for a particular value of A and T, interaction increases μ/μ_0 appreciably over its noninteracting value.

To obtain T_c from Eq. (14), we next calculate the specific heat using Eqs. (12) and (13). Calculated values of $C_A(T)/Ak_B$, for both interacting and noninteracting bosons with $A = 5\,000, 10\,000$, and $15\,000$, have been plotted against T (in nK) in Fig. 2. Once again, the general features are the same for both interacting and noninteracting cases. The heat capacity increases with T smoothly and becomes maximum at a particular $T = T_c$. Beyond that it drops suddenly, the drop being more sudden as A increases. $C_A(T)$ finally converges to $3Ak_B$ for large T. For condensates with repulsive interaction at $T > T_c$, very excited energy levels are also occupied with a small but nonvanishing probability. These are cut off in order to reduce the CPU time. As a result, the asymptotic parts of such curves in Fig. 2 do not converge properly. From Fig. 2, it is clear that although for small A, the curve is continuous at T_c, a conceived discontinuity in the slope of the heat capacity curve becomes gradually distinct as A increases, as predicted in the thermodynamic limit. From Fig. 2, it can also be seen that the effect of interaction on the heat capacity is relatively small, but it increases with A.

Transition temperature (T_c) is obtained numerically from the calculated C_A, using Eq. (14). In Table I, we present ground-state energy (in units of $\hbar\omega$) and T_c (in nK), calculated by the CPHE method, in the second and fifth columns respectively for selected values of A given in the first column. The third column lists the values of critical temperature (T_c^0) of noninteracting bosons in the thermodynamic limit, given by [6]

$$T_c^0 = \left[\frac{A}{\zeta(3)}\right]^{1/3} \frac{\hbar\omega}{k_B}, \tag{17}$$

where $\zeta(3)$ is the ζ function. In a typical laboratory condensates, there are lowerings of the critical temperature due to repulsive interaction, as also due to the finite-size effect [5]. In the fourth column, we present our calculated transition temperature (T_c') for noninteracting bosons in the same trap. The lowering due to finite-size effect ($T_c' - T_c^0$) is seen to be somewhat larger than the estimate given in Ref. [5]. The lowering of the transition temperature due to repulsive interaction, $\Delta T_c = T_c' - T_c$, is presented in the sixth column. It increases with increase in A, in agreement with the theory [5]. This lowering of T_c in a repulsive BEC can be intuitively understood to be due to the lowering of the peak density of the gas, as more of the particles are pushed upward into higher energy states. The repulsive interaction thus increases the energy of the system and therefore it must be cooled down to an even lower temperature, so that a macroscopic fraction of the particles can be in the ground state. The experimental values T_c^{exp} ($\approx 0.94 \times T_c^0$) [2] are presented in the seventh column. CPHE results for T_c are close to but smaller than the experimental values and the percentage difference is shown in the last column. The magnitude of the percentage difference gradually decreases as A increases.

Next we calculate the condensate fraction $A_0(T)/A$, where A_0 is the number of particles in the ground state at T. For the noninteracting Bose gas in the thermodynamic limit, it is given by [5] $\frac{A_0}{A} = 1 - (\frac{T}{T_c^0})^3$. The calculated condensate fraction for interacting condensates containing $A = 5\,000, 10\,000$, and $15\,000$ bosons are plotted as a function of T (in nK) in Fig. 3. The general nature is similar to that of the ideal Bose gas, although quantitative differences exist for the actual numerical values, showing the effects of realistic interatomic interaction and finite size. In the same figure, we also plot our calculated condensate fraction for the same number of

TABLE I. Ground-state energies and critical temperatures of the condensate containing different numbers (A) of ^{87}Rb atoms.

A	Ground-state energy ($\hbar\omega$)	T_c^0 (nK)	T_c' (nK) for noninteracting bosons	T_c (nK) for interacting bosons	ΔT_c (nK) due to interaction	$T_c^{\exp}$ (nK) expt. [2]	Difference (%) from expt.
5 000	20207.0053	60.03	55.81	55.06	−0.75	56.43	−2.43
7 000	31916.8493	67.16	62.87	62.01	−0.86	63.13	−1.77
9 000	44996.8594	73.03	68.87	67.79	−1.08	68.65	−1.25
11 000	59257.0459	78.08	73.96	72.71	−1.25	73.40	−0.94
13 000	74564.9947	82.55	78.78	77.18	−1.60	77.60	−0.54
15 000	90821.9956	86.58	83.53	81.12	−2.41	81.39	−0.33

noninteracting bosons. It is seen that noninteracting values of $\frac{A_0}{A}$ and transition temperature are larger than those for the corresponding repulsive condensate, although the difference is only a few percent. We next compare our results with other theoretical calculations and also with available experiments. Among the few many-body calculations of thermodynamical quantities reported so far, an important one is the path-integral Monte Carlo (PIMC) calcuation by Krauth [16], which was carried out for 10 000 bosons in the JILA trap. Hence for a comparison, we select $A = 10\,000$ and present $\frac{A_0}{A}$ calculated by the CPHE method as a function of $\frac{T}{T_c^0}$ in Fig. 4. Results of PIMC calculations and mean-field theory (MFT) estimates [5], and also experimental results [2], are also presented in the same figure. The experimental and PIMC results are obtained by digitally scanning Fig. 27 of Ref. [5]. The MFT curve is obtained from Eq. (122) of Ref. [5] with $\eta = 0.4$. From this figure, one notices that the CPHE results are closer to the experimental points than either the MFT or PIMC results. However, the differences are relatively small, while the experimental points scatter. Due to the experimental uncertainties, relative merits of different theoretical estimates is rather inconclusive at this stage. Nevertheless, all these theoretical estimates indicate a significant importance of interatomic interactions.

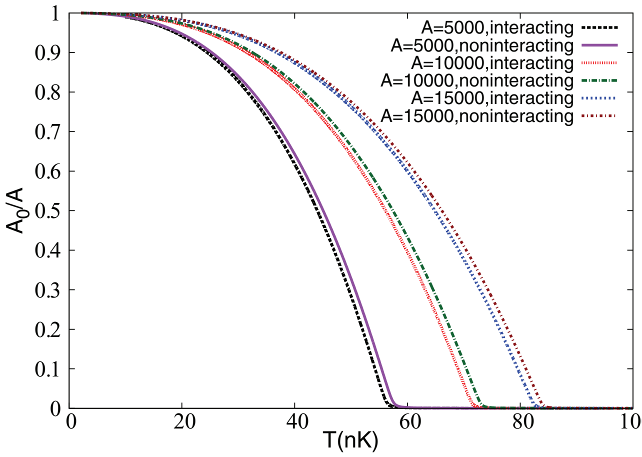

FIG. 3. (Color online) Plot of condensate fraction $A_0(T)/A$ calculated by CPHE method against T in nK for 5 000, 10 000, and 15 000 repulsively interacting bosons in the harmonic trap. The left, middle, and right pairs of closely spaced curves correspond to $A = 5\,000$, 10 000, and 15 000 respectively. Plots for noninteracting bosons are also included, which lie above the corresponding interacting curve for each closely spaced pair. This again shows that T_c decreases due to repulsive interaction.

However from Figs. 2, 3, and 4, it is clear that the effect of interaction on thermodynamic quantities is not too drastic for a dilute condensate, although ground-state energy (hence also μ) of the repulsive condensate increases by a large amount due to the interaction, and this amount increases rapidly with A (see Table I). Note that the ground-state energy of a noninteracting condensate containing A bosons in the trap is $1.5A\hbar\omega$ and the extremely rapid increase in the ground-state energy of the interacting condensate is due to the net interaction of all the pairs, which increases roughly as A^2. The average contribution of an interacting pair to the ground state of the condensate, $(E_{00} - 1.5A\hbar\omega)/[A(A-1)/2]$, is quite small ($\sim 6 \times 10^{-4}$ for $A = 15\,000$ ^{87}Rb atoms in the JILA trap). This quantity decreases with increasing A. This is understandable, since as A increases, the net repulsive interaction on a given particle pushes the particle outward, thus increasing the average interparticle separation. Although the ground-state energy of the condensate increases by a large amount due to interaction,

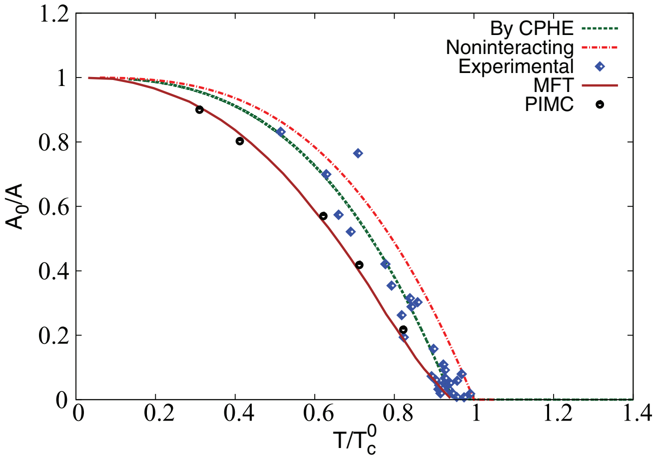

FIG. 4. (Color online) Plot of condensate fraction $A_0(T)/A$ calculated by CPHE method against T/T_c^0 for $A = 10\,000$ bosons in the harmonic trap (black dotted curve). Experimental results [2] (blue [gray] diamonds), path integral Monte Carlo (PIMC) results [16] (solid circles), and mean-field theory (MFT) estimates [5] (brown [dark gray] continuous curve) are also presented for comparison. Experimental and PIMC results have been obtained by digitally scanning Fig. 27 of Ref [5]. For $T < T_c$, the experimental points are closer to the CPHE results. Results for noninteracting bosons are shown by the dash-dotted (red [gray]) curve.

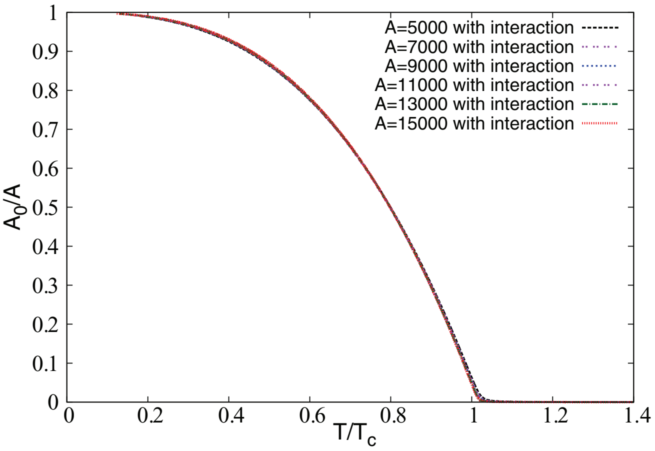

FIG. 5. (Color online) Plot of A_0/A against T/T_c for indicated number of interacting particles in the trap. All these curves, as well as plots for noninteracting particles, lie on a universal curve and are indistinguishable.

the effect of interaction on the excitation spectrum is much smaller [17]. Hence its effect on the thermodynamic quantities is also rather small.

We have noticed an interesting feature of the thermodynamic quantities. When a thermodynamic quantity per particle in a dimensionless unit is plotted against T/T_c, the plot appears to fall on a universal curve, independent of the number of particles in the condensate, regardless of whether they are interacting or noninteracting. We demonstrate this in Figs. 5 and 6, where we plot A_0/A and $C_A/(Ak_B)$ against T/T_c for different values of A, both interacting and noninteracting. It can be seen that, within calculational errors, all the curves of a particular thermodynamic quantity fall on a universal curve, *independent of A and interaction*.

In this spirit, in Fig. 7 we plot average energy per particle [calculated using Eq. (12)] as a function of T/T_c, for different particle numbers in the condensate. Once again, plots for interacting condensate for different A fall on a universal curve. However, the plots of noninteracting cases are indistinguishable for different A, but this curve for noninteracting bosons lie appreciably below the one for interacting bosons. This can be understood from Table I and the associated discussion. For $T < T_c$, the average energy per particle increases slowly with T. The rate of increase is slower than that of an ideal noncondensed Bose gas. This can be understood from the fact that a macroscopic fraction of the bosons in the condensate remains in the lowest energy state for $T < T_c$. For $T > T_c$, the average energy per particle approaches the classical limit of $3k_BT$, since at such temperatures, the Bose gas becomes noncondensed. The calculated result is similar to that obtained in Refs. [2,29].

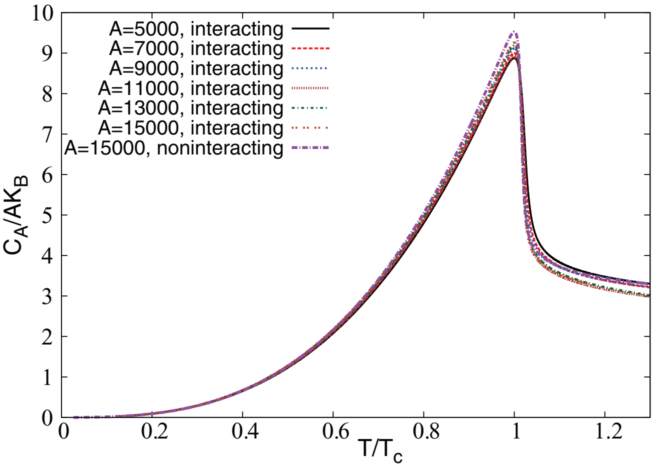

FIG. 6. (Color online) Plot of C_A/Ak_B against T/T_c for indicated number of interacting and noninteracting particles in the trap. The curves from bottom to top, on the left side up to the peak, correspond to $A = 5\,000, 7\,000, 9\,000, 11\,000, 13\,000, 15\,000$ interacting bosons and $A = 15\,000$ noninteracting bosons respectively. The curves nearly overlap, except for T/T_c close to 1. The divergence for $T/T_c > 1.05$ is due to incomplete convergence in the numerical calculation.

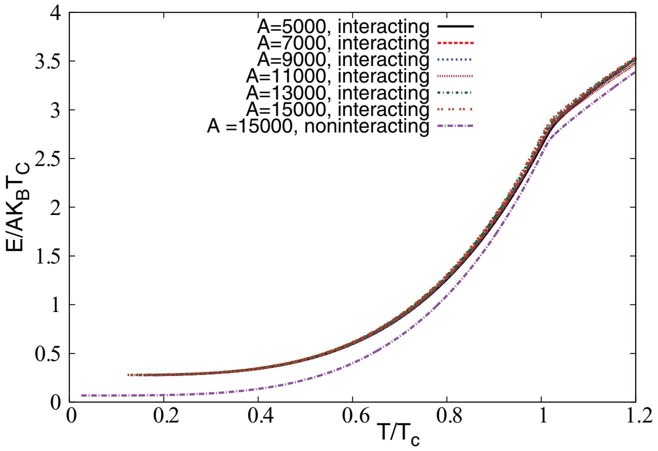

FIG. 7. (Color online) Plot of average energy per particle of the condensate against T/T_c for indicated number of interacting bosons in the harmonic trap. Although plots for all interacting cases fall on a universal curve, those for the noninteracting bosons fall on a *different universal* curve. As an example, a plot for $A = 15\,000$ noninteracting bosons is included as long dash-dotted (pink [gray]) curve.

Next we have calculated the average entropy per particle (S/Ak_B) using Eq. (15) and the results are plotted against T/T_c

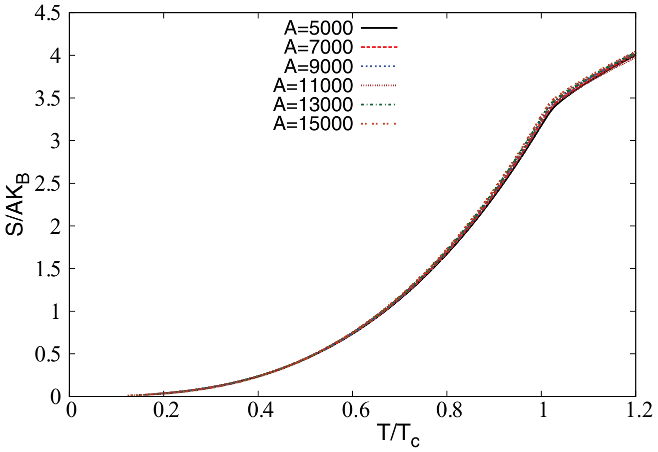

FIG. 8. (Color online) Plot of average entropy per particle against T/T_c for indicated number of interacting bosons in the harmonic trap. These curves, similar to the ones for noninteracting bosons, lie on a universal curve and are indistinguishable.

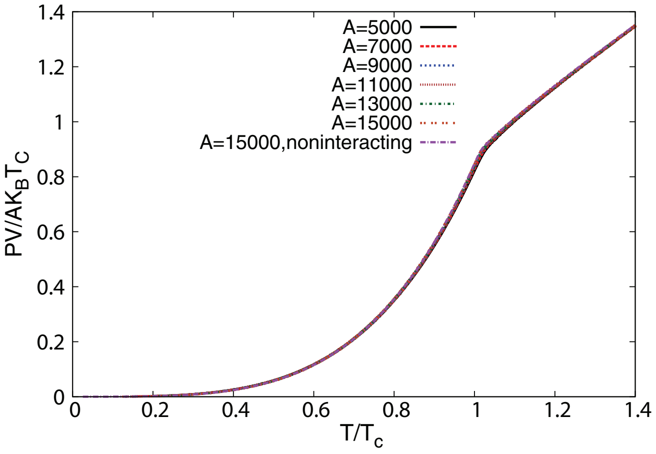

FIG. 9. (Color online) Plot of PV/Ak_BT_c against T/T_c for indicated number of interacting and noninteracting bosons in the harmonic trap. All the curves lie on a universal curve and are indistinguishable.

in Fig. 8. Only the particles in the excited states contribute to the entropy of the system. From Fig. 5, we notice that for a given value of T/T_c, the fraction of particles in the excited states (A_{ex}/A) is almost independent of A. Hence S/Ak_B is also practically independent of A. This explains the universal nature of this curve. The same argument holds for the universal nature of the energy per particle (Fig. 7) and heat capacity per particle (Fig. 6). The overall nature of both the average energy and entropy per particle are similar to those found in Ref. [29], which, however, considered a condensate of only 200 particles in a cubical box, with a different interaction strength.

Finally we have calculated the thermodynamic quantity PV/Ak_BT_c using the relation given in Eq. (16). Figure 9 shows the variation of this quantity as a function of T/T_c. For $T > T_c$, the system satisfies the classical relation $PV = Ak_BT$, as expected. It is seen from Figs. 5–9 that each of the quantities plotted as a function of T/T_c falls to within numerical errors, on a universal curve (independent of A or interaction) for that quantity. For the avarage energy per particle, the curves are independent of A, but are different for interacting and noninteracting bosons.

IV. SUMMARY AND CONCLUSION

The principal objective of this work has been to investigate the effects of interaction on the thermodynamic properties of a repulsively interacting Bose gas containing a large but finite number of bosons confined in a harmonic oscillator trap. The importance of this study stems from the fact that although thermodynamics properties of a noninteracting Bose gas in a harmonic trap are well studied theoretically, not much attention has been paid to thermodynamics of interacting bosons. We solve the many-body problem of atoms interacting via the realistic van der Waals potential by the correlated potential harmonics expansion (CPHE) method. This technique uses the potential harmonics expansion basis, which is a subset of the full hyperspherical harmonics basis and retains only two-body correlations. It is justified since the laboratory condensates are designed to be very dilute, in order that three-body collisions (which lead to molecule formation and consequent depletion of the condensate) are absent in the trapped gas. Hence only two-body correlations are relevant. Use of this subset reduces the complexity of the full many-body problem dramatically, so much so that a system containing a large number of interacting particles becomes manageable. We also include a short-range correlation function, which is chosen to be the solution of the zero-energy two-body Schrödinger equation with its asymptotic behavior corresponding to the experimental s-wave scattering length a_s. This short-range correlation function incorporates the correct short-range behavior of the interacting pair Faddeev component, and also guarantees that the effective atom-atom potential corresponds to the experimental a_s. In addition, it improves the convergence rate of the chosen expansion basis. The CPHE method has been successfully applied to zero-temperature static properties of both repulsive and attractive condensates.

We have calculated the transition temperature (T_c) and the temperature dependence of the chemical potential, heat capacity, condensate fraction, energy, entropy, and pressure (in the form of PV/k_BT_c) of a Bose gas containing A atoms of ^{87}Rb in the original JILA trap. For a finite A, there is no critical temperature at which there is a sudden change of phase. Instead, temperature dependence of each thermodynamic quantity shows a rather rapid—although continuous—change in behavior at a temperature T_c, which we define as the transition temperature. We adopt the definition of T_c as the temperature at which heat capacity(C_A) attains a maximum. We find that T_c is a few percent less than the experimental value $\approx 0.94T_c^0$ [2], where T_c^0 is the corresponding critical temperature for the ideal Bose gas in the thermodynamic ($A \to \infty$) limit. The calculated chemical potential is found to decrease very slowly for $T < T_c$, but then rapidly for $T > T_c$. Next our calculated heat capacity, energy, entropy, and PV/k_BT_c per particle increase with T, initially slowly and then rapidly near T_c for $T \leqslant T_c$. The nature of T dependence changes radically but continuously across T_c. For $T > T_c$, the thermodynamic quantities attain their classical, nearly ideal Bose gas values. The $T > T_c$ behavior is understandable in the following manner. For $T > T_c$, all the bosons are in higher energy levels, which are much more extended spatially. The peak central density now vanishes and atoms are distributed thermally. Due to the increased average interparticle separation, the interatomic interaction becomes less important and the ideal Bose gas result is approached as T increases.

As a further comparison with other theoretical estimates and experiment, we plotted the condensate fraction calculated by CPHE method along with the mean-field theory (MFT) estimate [5], the results of path integral Monte Carlo (PIMC) calculation [16], and experimental points [2]. We find that the CPHE results are somewhat nearer to the experimental points, but due to scattering of the experimental points a definite conclusion regarding the relative merits is not possible at this sage. One can only say that the condensate fractions of a finite and repulsively interacting condensate calculated by different many-body methods are close to each other, and are somewhat smaller than the experimental points. However, there is a significant difference from the noninteracting values, showing the importance of interactions.

Our calculations indicate that for large A, the effect of interatomic interaction is quite drastic on the total energy of the ground and excited states of the many-body system (Table I). This is understood by the fact that the net energy increases due to $A(A-1)/2$ interacting pairs. However, as A increases, the average contribution to energy by *a single interacting pair* decreases slowly, since the net repulsion of all the pairs pushes the particles outwards, increasing the average separation. On the other hand, the Bose distribution function, which controls the temperature dependence of thermodynamic quantities, depends on the difference of the total energy of a state ($E_{\rm nl}$) and the chemical potential [$\mu(T)$]. This difference (as also the *excitation energies* [17]) do not depend *too strongly* on the interaction, since the net repulsion affects each energy level (and hence the chemical potential, which is slightly less than the ground-state energy for $T < T_c$) roughly equally. As a result the effect of interactions on the thermodynamic quantities is not too drastic, although that on the energy of the system is quite large.

In the process of our calculations, we have noticed an interesting feature. We find that each of the thermodynamic quantities per particle expressed in a dimensionless unit, when plotted against T/T_c, falls on a universal curve for that quantity. The universal curve does not depend on A and on whether the bosons are interacting or not (except for the average energy per particle of the noninteracting condensate). Thus one can obtain a particular thermodynamic quantity at a temperature T for the condensate containing any number of interacting or noninteracting particles, knowing the universal curve for that quantity and T_c (which depends on A and the two-body interaction). This corresponds to the scaling behavior of the Bose-Einstein condensates [5].

We conclude from this many-body study that the effect of a repulsive interaction is quite substantial on the energies of the collective states of the condensate, but is much less pronounced on the collective excitations or on the thermodynamics of the system. Hence the many-body results for the thermodynamic quantities differ from the results derived from the mean-field GP equation by only a few percent. We provide a microscopic explanation of this observation based on our many-body theory, as explained above. We also observe the scaling behavior satisfied by the many-body results of the condensate.

ACKNOWLEDGMENTS

We acknowledge the financial support of University Grants Commission, India, under a Major Research Project [F. No. 40-439/2011(SR)]. T.K.D. thanks the Department of Science and Technology (DST), Government of India, for financial support.

[1] M. H. Anderson, J. R. Ensher, M. R. Matthews, C. E. Wieman, and E. A. Cornell, Science **269**, 198 (1995).

[2] J. R. Ensher, D. S. Jin, M. R. Matthews, C. E. Wieman, and E. A. Cornell, Phys. Rev. Lett. **77**, 4984 (1996).

[3] C. C. Bradley, C. A. Sackett, and R. G. Hulet, Phys. Rev. Lett. **78**, 985 (1997).

[4] K. B. Davis, M.-O. Mewes, M. R. Andrews, N. J. van Druten, D. S. Durfee, D. M. Kurn, and W. Ketterle, Phys. Rev. Lett. **75**, 3969 (1995).

[5] F. Dalfovo, S. Giorgini, L. P. Pitaevskii, and S. Stringari, Rev. Mod. Phys. **71**, 463 (1999).

[6] C. J. Pethick and H. Smith, *Bose-Einstein Condensation in Dilute Gases* (Cambridge University Press, Cambridge, 2002).

[7] V. Romero-Rochin, J. Phys. Chem. **109**, 21364 (2005).

[8] V. I. Yukalov, Laser Phys. Lett. **1**, 435 (2004).

[9] M. O. Mewes, M. R. Andrews, N. J. van Druten, D. M. Kurn, D. S. Durfee, and W. Ketterle, Phys. Rev. Lett. **77**, 416 (1996).

[10] N. Sandoval-Figueroa and V. Romero-Rochin, Phys. Rev. E **78**, 061129 (2008).

[11] D. Blume and C. H. Greene, Phys. Rev. A **63**, 063601 (2001).

[12] T. K. Das, S. Canuto, A. Kundu, and B. Chakrabarti, Phys. Rev. A **75**, 042705 (2007).

[13] T. K. Das and B. Chakrabarti, Phys. Rev. A **70**, 063601 (2004).

[14] S. Goswami, T. K. Das, and A. Biswas, Phys. Rev. A **84**, 053617 (2011).

[15] S. A. Sofianos, T. K. Das, B. Chakrabarti, M. L. Lekala, R. M. Adam, and G. J. Rampho, Phys. Rev. A **87**, 013608 (2013).

[16] W. Krauth, Phys. Rev. Lett. **77**, 3695 (1996).

[17] A. Biswas and T. K. Das, J. Phys. B **41**, 231001 (2008).

[18] S. Giorgini, L. P. Pitaevskii, and S. Stringari, Phys. Rev. A **54**, R4633 (1996); Phys. Rev. Lett. **78**, 3987 (1997).

[19] T. K. Das, A. Kundu, S. Canuto, and B. Chakrabarti, Phys. Lett. A **373**, 258 (2009).

[20] J. L. Ballot and M. Fabre de la Ripelle, Ann. Phys. (N.Y.) **127**, 62 (1980).

[21] M. Fabre de la Ripelle, Ann. Phys. (N.Y.) **147**, 281 (1983).

[22] M. Abramowitz and I. A. Stegun (eds.), *Handbook of Mathematical Functions* (Dover, New York, 1972).

[23] A. Biswas, B. Chakrabarti, T. K. Das, and L. Salasnich, Phys. Rev. A **84**, 043631 (2011).

[24] B. Chakrabarti, T. K. Das, and P. K. Debnath, Phys. Rev. A **79**, 053629 (2009); A. Biswas, J. Phys. B **42**, 215302 (2009); A. Biswas, B. Chakrabarti, and T. K. Das, J. Chem. Phys. **133**, 104502 (2010); S. K. Haldar, B. Chakrabarti, and T. K. Das, Phys. Rev. A **82**, 043616 (2010); A. Biswas, T. K. Das, L. Salasnich, and B. Chakrabarti, *ibid.* **82**, 043607 (2010); P. K. Debnath and B. Chakrabarti, *ibid.* **82**, 043614 (2010).

[25] T. K. Das, H. T. Coelho and M. Fabre de la Ripelle, Phys. Rev. C **26**, 2281 (1982).

[26] V. P. Brito, H. T. Coelho, and T. K. Das, Phys. Rev. A **40**, 3346 (1989); T. K. Das, H. T. Coelho, and V. P. Brito, Phys. Rev. C **48**, 2201 (1993); R. Chattopadhyay and T. K. Das, Phys. Rev. A **56**, 1281 (1997); T. K. Das and B. Chakrabarti, Phys. Rev. E **62**, 4347 (2000).

[27] K. Huang, *Statistical Mechanics*, 2nd ed. (Wiley, New York, 1987).

[28] R. Napolitano, J. De Luca, V. S. Bagnato, and G. C. Marques, Phys. Rev. A **55**, 3954 (1997).

[29] K. E. Dorfman, M. Kim, and A. A. Svidzinsky, Phys. Rev. A **83**, 033609 (2011).